2022 年臺灣國際科學展覽會
優勝作品專輯

作品編號 **100040**

參展科別 **工程學**

作品名稱 **Development of an Audio Modulated Tesla Coil**

得獎獎項 **一等獎**

青少年科學獎

國　　家 **Switzerland**

就讀學校 **Kantonsschule Wettingen**

指導教師

作者姓名 **Maz Wegmuller**

關鍵詞 **Tesla coil, Transformer, high voltage**

作者照片

1 Introduction

To understand what a Tesla coil is, what it is used for and why it exists, it is necessary to look at the history of its creation in a historical context.

Nikola Tesla was born in 1856 in Croatia and was one of the most important scientific researchers in the 19th and 20th centuries. It was precisely at this time that industrialization and the subsequent electrification of industry and households began in the USA. Tesla was a visionary and developed, among many other revolutionary innovations, a **wireless power transmission** system, new **messaging systems**, and induction motors, and believed in the potential of **alternating current power transmission**.[1]

Nikola Tesla had a vision and wanted to use his invention to supply the **whole world with wireless electricity**. This way, there would be no need to build a power grid and mobile devices would never have to be charged. Today we know that this vision will not become reality in the foreseeable future, because all wireless power transmission systems are subject to large losses. Tesla tried to realize his vision with his new invention, the **Tesla coil or Tesla transformer**. In 1891, Tesla filed the first plans of this high voltage generator with the US Patent Office.[2]

The Tesla coil is basically a high-voltage transformer that generates impressive discharges and transmits energy through the air. Nikola Tesla even built a nearly 60-meter Tesla coil on Long Island in the U.S. that was to be used for wireless power transmission and messaging. However, the so-called **Wardenclyffe Tower** never worked and was torn down again after about 10 years.[3]

Unfortunately, Nikola Tesla was not aware that his vision would probably never be possible. Nevertheless, many existing power transmission systems today are based on principles similar to those discovered by Nikola Tesla over 100 years ago. However, the Tesla coil had no future and was never used in industry, in the power grid or for message transmission. Today, the Tesla coil is mainly used for **research purposes** and as a **display object**. It can be found in **museums**, at **universities** and **colleges**. Students can learn very well from a Tesla coil how exactly the complex electrotechnical processes work.[4]

---

[1] „Nikola Tesla“, Who’s who, https://whoswho.de/bio/nikola-tesla.html, 22.11.2021.
[2] Tesla Nikola, „System Of Electric LIghting“, Google Patents, https://patents.google.com/patent/US454622, 12.10.2020.
[3] „Tesla's Tower at Wardenclyffe“, Tesla Science Center, https://teslasciencecenter.org/history/tower/, 22.11.2021.
[4] „Teslaspule: Geschichte, Funktionsprinzip, Anwendung“, hilfreich.de, http://www.hilfreich.de/teslaspule-geschichte-funktionsprinzip-anwendung_7868, 22.11.2021.

However, the Tesla coil additionally generates beautiful discharges, which have always fascinated many people. As a result, a community of electrical engineers and hobbyists formed, who constantly developed and improved the original Tesla coil of Nikola Tesla. The first Tesla coil of Nikola Tesla is today called **SGTC (Spark Gap Tesla Coil).** The SGTC is a very rudimentary Tesla coil that discharges through a physical spark gap. Today, there are various types of semiconductor-controlled Tesla coils that were developed in the 1980s. One of the first semiconductor controlled, rather low power Tesla coils is called **SSTC (Solid State Tesla Coil).** The SSTC has only one oscillating circuit. The electronics usually automatically adjust to the resonant frequency of the one resonant circuit. However, the first **Dual Resonant Solid State Tesla Coils (DRSSTC)** were not developed and documented until around 2005. It wasn't until the DRSSTC that it had similar performance to the SGTC and could be driven very precisely. DRSSTC means semiconductor-controlled Tesla coil with two resonant frequencies. Unlike Nikola Tesla's SGTC, the DRSSTC is controlled by high-precision and high-performance semiconductors. Because it has two complete resonant circuits, it also has two resonant frequencies that are tuned to each other. From these two resonant frequencies the DRSSTC also gets its name. Due to the digital and very precise control of the semiconductors, it can even be audio modulated.[5]

The high-power transistors (IGBT) are driven in such a way that audible pressure waves, and thus music, are generated by the electrical discharges at the high-voltage electrode.

In the context of this work, the two questions were:

- How is a DRSSTC **developed and built**?
- How do you measure an electrical voltage of **200,000 V**, which changes sign more than **100,000 times per second**?

[5] McCauley Daniel, *DRSSTC Building the Modern Day Tesla coil* (United States of America: Lulu Press, 2006), S. 16.

2 Operation of a DRSSTC

DRSSTC stands for Dual Resonant Solid State Tesla Coil. Their special feature is that their power electronics consist of **two magnetically coupled resonant circuits**, the primary and secondary resonant circuits. Figure 1 shows a schematic representation of the resonant circuits as they appear in DRSSTCs. Once the primary resonant circuit is set into forced oscillation, current flows through the primary coil L_{pri} at its resonant frequency. Due to the changing magnetic field of L_{pri}, an energy exchange takes place to the secondary coil L_{sec}. This is *Faraday's law of induction*.[6]

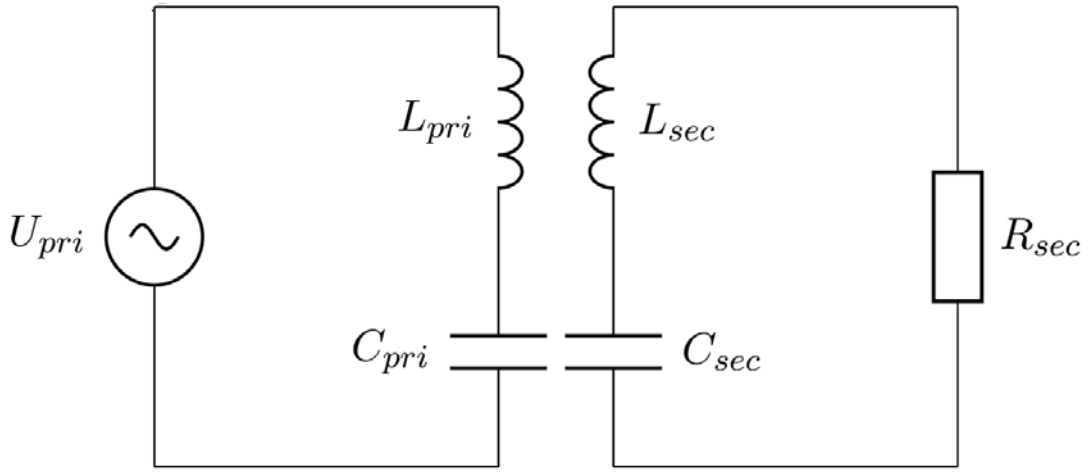

Figure 1: Magnetically coupled primary and secondary resonant circuit via inductances L_{pri} and L_{sec}.

The **resonant frequency** of the oscillating circuit can be calculated with this formula, where L_{pri} stands for the inductance of the primary coil and Cpri for the capacitance of the primary capacitor:[7]

$$f_{res} = \frac{1}{2\pi\sqrt{L_{pri}C_{pri}}}$$

The high voltages are visible in a Tesla transformer at the so-called topload. From the topload, the voltage discharges into the environment. In theory, the capacitance of the discharge electrode with respect to the environment corresponds to the secondary capacitance C_{sec}. To generate a discharge at the topload, very high voltages and currents must flow on the secondary side. To achieve this, the primary and secondary resonant circuits are operated in resonance and the turns-to-number

[6] Albach Manfred, *Elektrotechnik* (München: Pearson Deutschland GmbH, 2020), S. 263.
[7] Albach Manfred, *Elektrotechnik* (München: Pearson Deutschland GmbH, 2020), S. 375.

ratio is selected so that **high currents flow on the primary** side and the **voltage is high on the secondary** side. The high currents in the primary resonant circuit are achieved by applying a constant voltage in terms of magnitude across the series resonant circuit, consisting of L_{pri} and C_{pri}, and changing its sign with the resonant frequency of the LC resonant circuit. This forced oscillation causes a voltage overshoot in the primary resonant circuit, which in turn causes strong currents to flow. The square wave signal in Figure 2 shows the change in applied voltage across the primary resonant circuit. The violet curve shows the increase in the secondary voltage until a discharge occurs.[8]

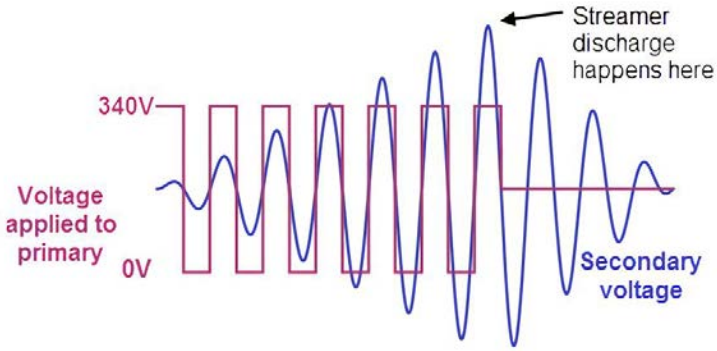

Figure 2: Primary and secondary voltage.

To precisely control the square wave voltage, the 50 Hz mains voltage with the voltage rms value of 230 V must first be converted to a **DC voltage**.

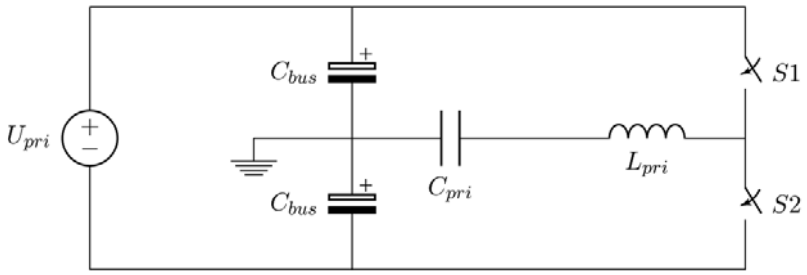

Figure 3: Primary oscillating circuit with C_{bus} as DC voltage source and the switches S1 and S2, which switch it via the oscillating circuit.

In Figure 3, switches S1 and S2 are responsible for changing the sign of the voltage across the LC resonant circuit. In reality, **IGBTs**, short for Insulated-Gate Bipolar Transistors, are used as switches. These semiconductor modules change from a blocking state to a conducting state and the voltage from C_{bus} is applied across the oscillating circuit with different signs. Under no circumstances are both switches or

[8] Gadola Robin, Stamm Jonas, Uschatz Cédric, *Entwicklung der Gate-Treiber Stufe für eine Audiomodulierte Teslaspule*, Gruppenarbeit Herbstsemester 16/17, ETH Zürich, S. 1.

IGBTs turned on at the same time, they always alternate with each other. The sign of the applied voltage is changed in this way.

To protect the semiconductors, the oscillating circuit must be operated with a duty cycle of less than 10 %. This interrupts the forced oscillation and thus the operation of the coil at a certain frequency. The **frequency of the duty cycle is within the audible spectrum** and can be specified by a signal input. This thus allows sequential tones to be played and generated at different frequencies.[9]

In the **schematic diagram of a DRSSTC** on Figure 4, the power flow can be traced from the socket to the discharge. The Input Power Control regulates the current flowing into the DC Power Supply. The DC Power Supply are electrolytic capacitors. The Self-Resonant Driver (gate driver) is like a computer that monitors the whole system (with feedback transformers) and turns off the Tesla coil when needed. The Self-Resonant Driver controls the Switching Circuit. The switching circuit is the transistors, which in turn switch the DC power supply at the resonant frequency of the tesla coil via the primary resonant circuit.

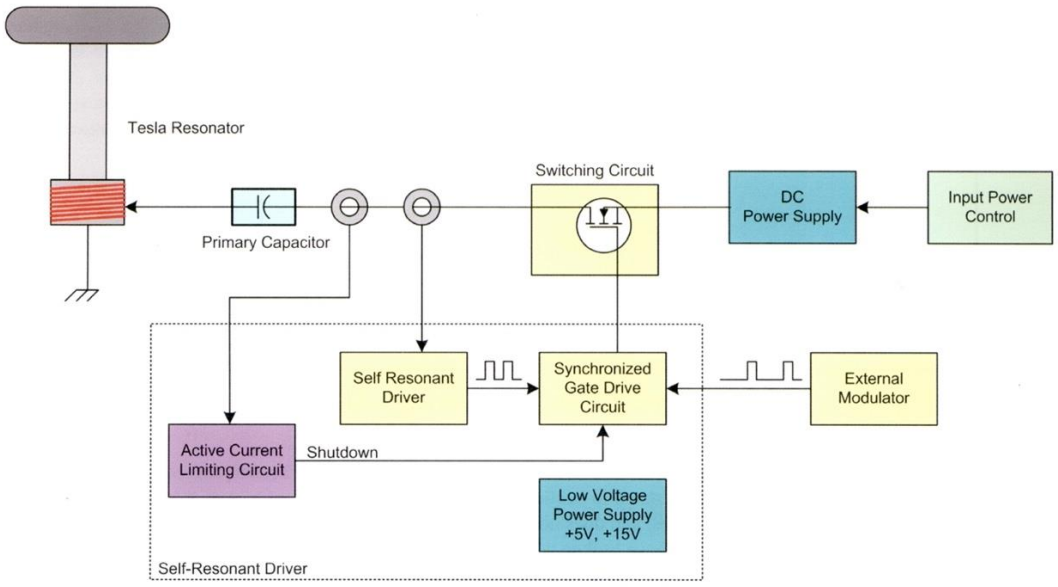

Figure 4: Schematic representation of a DRSSTC.

[9] Gadola Robin, Stamm Jonas, Uschatz Cédric, *Entwicklung der Gate-Treiber Stufe für eine Audiomodulierte Teslaspule*, Gruppenarbeit Herbstsemester 16/17, ETH Zürich, S. 1.

3 Engineering Process

In this part, the **planning, development and construction** of the DRSSTC is explained. First, however, a simulation was created to better estimate the resulting voltages and currents. The Tesla coil consists of different modules that all have to work together perfectly. Each module must be perfectly matched to all the others and only then can they work together optimally as a whole in a system. In this short summary, we will only explain the four most important modules and how they interact with each other. The final developed DRSSTC can be seen in figure 5.

All measurements in this paper were created using **Keysight's DSOX1204G, 200 MHz, 2 GSa/s oscilloscope**. In addition, the signal generator of this oscilloscope was always used.

Figure 5: An audio modulated DRSSTC with medium power output.

3.1 Simulation

To obtain a rough estimate of the resulting **currents and voltages in the primary and secondary resonant circuits**, a simple simulation with the program *LTspice XVII from Analog Devices* was used.[10] The simulation in Figure 6 was provided by ETH Zurich and adapted with the appropriate specifications.

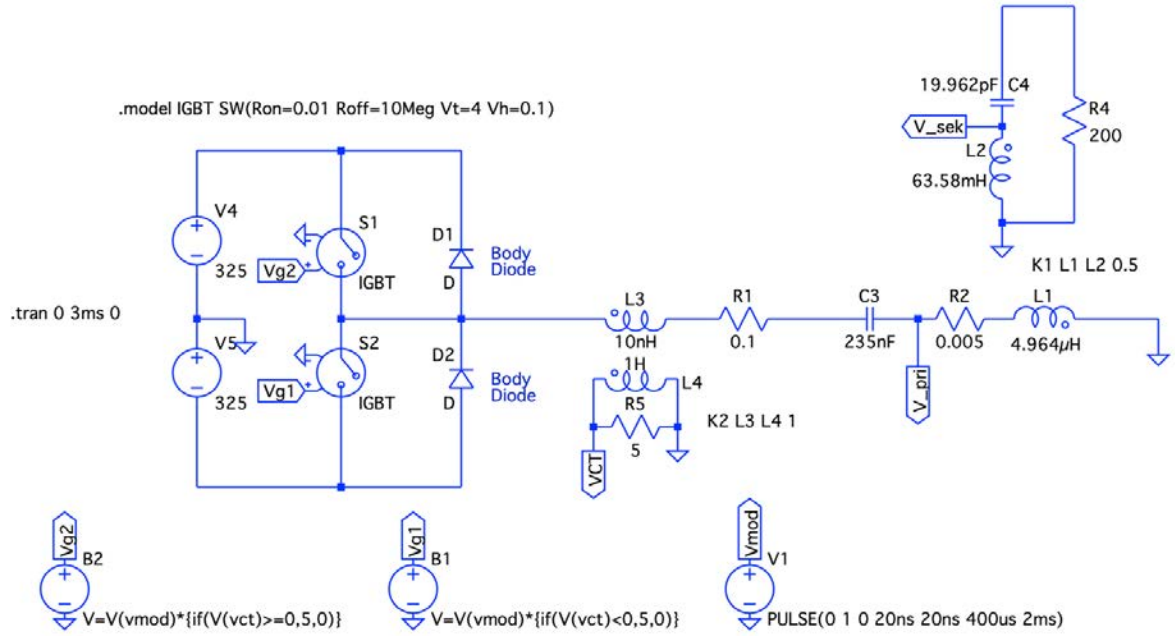

Figure 6: Simple LTspice simulation of a DRSSTC with half-bridge circuit.

The resonant frequency is about 145 kHz, as in the real system, defined by the inductance and capacitance of L1 and C3. The resonant circuit is supplied with two ideal voltage sources. They each have a DC voltage of 325 V and are designated V4 and V5 in Figure 6. The half-bridge arrangement of IGBTs is switched at the resonant frequency and driven 180° out of phase with each other. They are switched exactly in the current zero crossing. The diodes D1 and D2 must be added explicitly in the **LTspice simulation**. In commercial IGBT modules, the so-called body diodes are intrinsically installed. They conduct the current in reverse direction, so that the IGBTs are not damaged by overvoltage. When high currents are switched, a voltage is induced in the current conductor as the surrounding magnetic field collapses. Such a self-induced voltage is called self-induction and triggers so-called *voltage transients*.[11] Resistors R1 and R2 serve to dampen oscillations as they occur in

[10] „LTspice“, Analog Devices, https://www.analog.com/en/design-center/design-tools-and-calculators/ltspice-simulator.html, 22.10.2020.
[11] Albach Manfred, *Elektrotechnik* (München: Pearson Deutschland GmbH, 2020), S. 268.

reality due to the given resistance of the coils and connections. L4 measures the current in the primary oscillation circuit and passes the signal to the three functions at the bottom of the simulation. The signal through the voltage source V1 finally drives the IGBTs. The secondary resonant circuit at the top right of the simulation is magnetically coupled to the primary resonant circuit. The adjustable coupling factor tells how much of the magnetic flux from the primary coil flows through the secondary coil. It defines the energy exchange between the coils.[12]

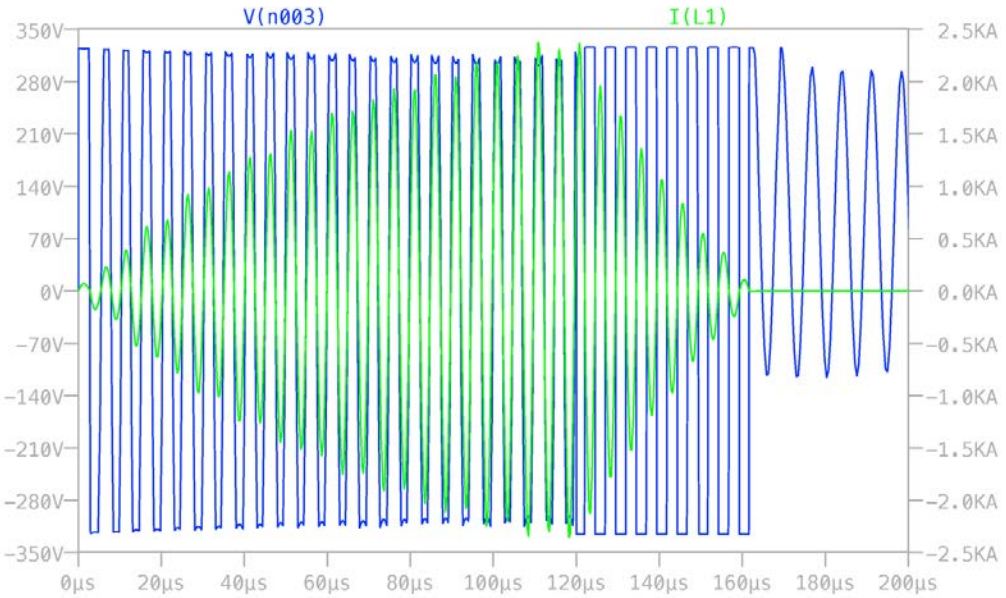

Figure 7: The DC voltage in blue keeps on swaying the sinusoidal current through the primary coil in green.

The blue curve in figure 7 shows the periodic polarity reversal of the DC voltage of ± 325 V across the oscillating circuit. This results in an increasing amplitude of the current and the voltage. The phenomenon that occurs can be compared to the **bumping of a swing**: The swing continues to swing out and the total energy of the swing increases as it is bumped into resonance. Further simulations showed that primary voltages with an amplitude of up to **10 kV** are reached and primary currents of **3 kA** flow through the oscillating circuit at an excitation of 400 µs. When building the power electronics, the components had to be designed for up to 10 kV and 3 kA.

[12] Gadola Robin, Stamm Jonas, Uschatz Cédric, *Entwicklung der Gate-Treiber Stufe für eine Audiomodulierte Teslaspule*, Gruppenarbeit Herbstsemester 16/17, ETH Zürich, S. 5.

3.2 Primary and secondary resonant circuit

The oscillating circuits each consist of an inductance and a capacitance. Especially the primary and secondary inductance remind of an ordinary transformer. However, this is a so-called air core coil since no ferromagnetic core is used. Another special feature of the coils of a Tesla transformer is that the winding ratio is very high. While the primary coil consists of about 4 windings, there are about 1'600 windings on the secondary side. Among other things, this very large ratio ultimately leads to the high voltages on the secondary side. The finished composition of the conspicuous oscillating circuits can be seen in Figure 8.[13]

Figure 8: The DRSSTC with the eye-catching and characteristic secondary coil.

3.3 Gate Driver

The gate driver is the **central control and monitoring unit** of the DRSSTC. It controls the transistors so that the primary oscillating circuit can be set into oscillation. It is also responsible for monitoring the primary current and switches off the transformer at a defined overcurrent.[14]

[13] Bell Steve, „Secondary Coil“, DeepFriedNeon, http://deepfriedneon.com/tesla_secondary.html, 3.10.2020.
[14] Ward Steve, „New DRSSTC Driver (2008 and now 2009)“, SteveHV, https://www.stevehv.4hv.org/new_driver.html, 13.10.2020.

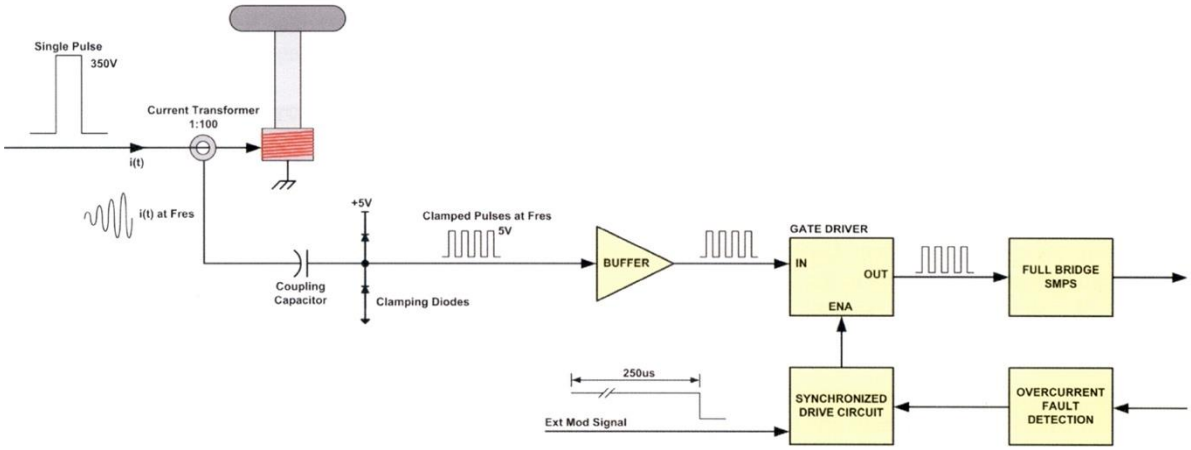

Figure 9: Basic operation of the gate driver in schematic representation.

Figure 9 shows the **basic operation of a gate driver**. It measures the resonant frequency with the gray current transformer and delays the signal through the buffer. Based on this input signal, the gate driver sends the control signal to the gates of the transistors and puts them either in the conducting or blocking state. When the interrupt signal ends or an overcurrent is detected, the gate driver turns off the transistors in the upcoming zero current crossing. The most important step for a reliable and high-performance tesla transformer is a robust and well-functioning gate driver.

Over 10 years ago, Steve Ward developed the **first DRSSTC driver**. It possessed the key requirements for a gate driver and was implemented in the first circuit he called Universal Driver, or UD.[15] Its improved version, the UD1.3b, has established itself as a robust and reliable standard gate driver to this day, displacing virtually all other gate drivers.

Over the years, the original gate driver has been continuously **improved and developed** by the Tesla coil community. The schematics and documentation of each gate driver are freely available.[16]

Nowadays, the most popular and reliable version is the **UD 2.7C by Gao Guangyan**.[17] The UD 2.8 developed in this work represents a slightly modified version of the UD 2.7C. The concrete schematic of the new UD 2.8, shown on Figure 10, can be found in the appendix of this thesis.

[15] Ward Steve, „New DRSSTC Driver (2008 and now 2009)“, SteveHV, https://www.stevehv.4hv.org/new_driver.html, 13.10.2020.
[16] Guangyan Gao, „UD 2.7“, Loneoceans, https://www.loneoceans.com/labs/ud27/, 12.10.2020.
[17] a. a. O.

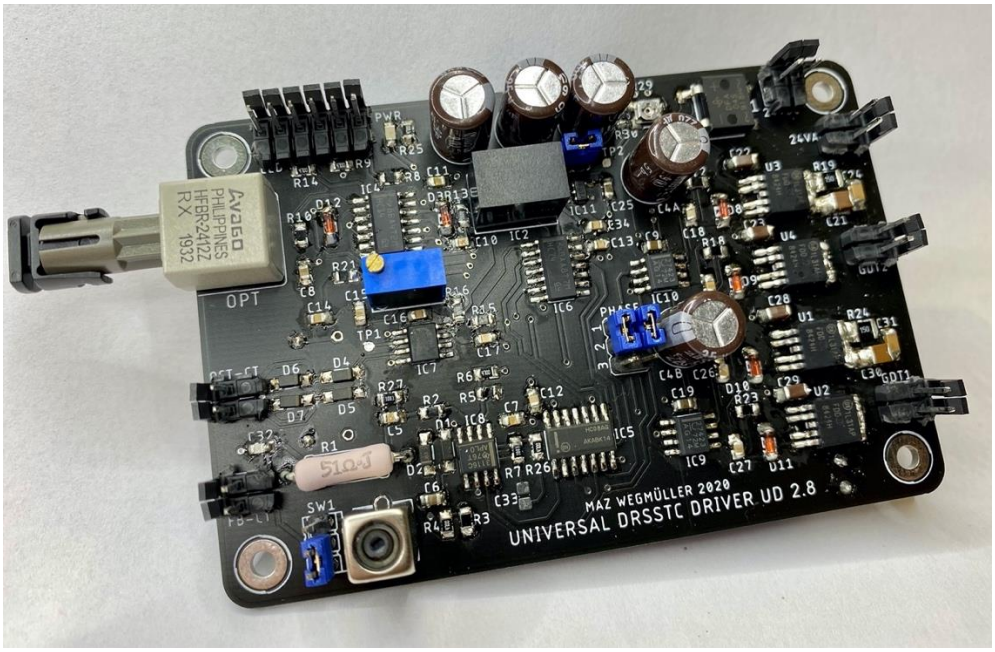

Figure 10: The completely assembled UD 2.8 on the self-designed circuit board.

3.4 IGBT Module

The IGBTs in a DRSSTC act as **inverters** and generate a square wave AC voltage for the primary resonant circuit.

For this DRSSTC, the **CM300DY-24H IGBT** half-bridge module from Powerex was used.[18] The CM300DY-24H, shown in Figure 11, has proven to be a reliable IGBT for DRSSTCs and was therefore chosen for this work.[19]

Figure 11: A CM300DY-24H IGBT half bridge module from Powerex.

[18] „CM300DY-24H“, Digi-Key Electronics, https://www.digikey.com/en/products/detail/powerex-inc/CM300DY-24H/1996275, 26.10.2020.
[19] Barnkob Mads, „IGBT selection for Tesla coils or ZCS inverters“, Kaizer Power Electronics, http://kaizerpowerelectronics.dk/tesla-coils/drsstc-design-guide/igbts/, 26.10.2020.

The CM300DY-24H is already an **IGBT half-bridge module** in which two individual IGBTs are installed. This compact form results in less parasitic inductances.

The IGBT half-bridge module can switch sustained currents of up to 300 A. Because currents in excess of 300 A are quickly switched in a DRSSTC, this is a problem. As in the Figure 7 simulation, currents as high as 3 kA can occur if the circuit is not limited. For this reason, the gate driver always **switches the IGBTs at zero current**. Thus, the CM300DY-24H IGBT can switch currents of up to 1 kA. The IGBT was mounted on a heat sink and connected to the rest of the components as shown in Figure 12.[20]

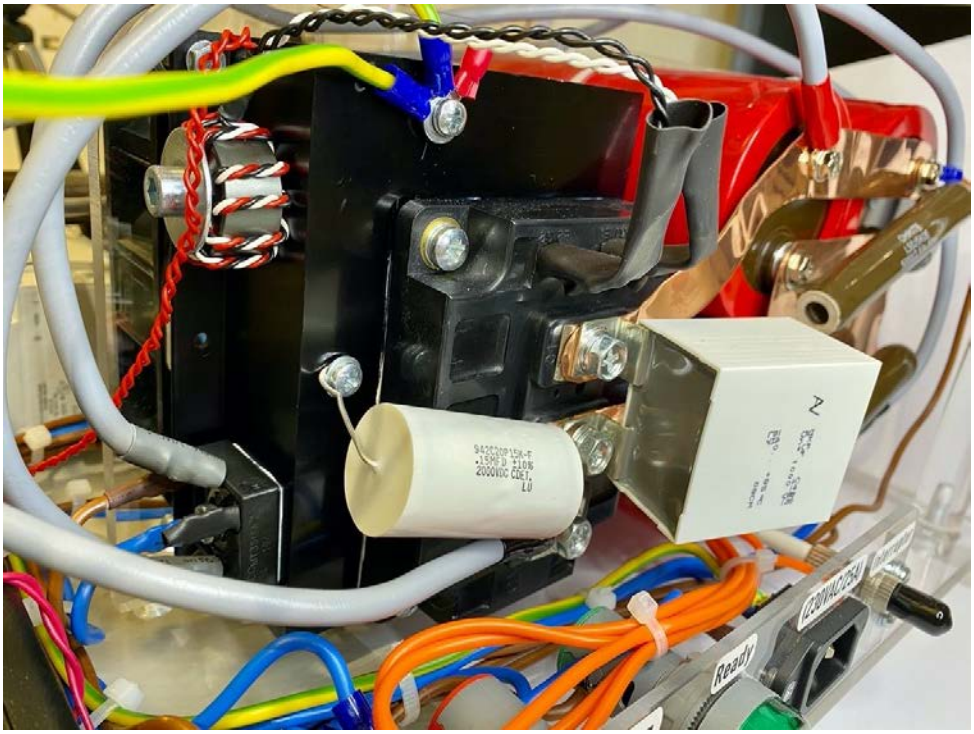

Figure 12: The CM300DY-24H IGBT module mounted on the grounded heat sink.

3.5 Interrupter

When the IGBT half-bridge permanently sets the primary oscillating circuit into a forced oscillation, high currents are generated within a very short time. To prevent the components from being overloaded by excessive voltages and currents, the Tesla transformer is not operated in a continuous wave mode but is **continuously interrupted at a clock frequency**. For this constant interruption, as the name already says, the interrupter is responsible.

[20] Barnkob Mads, „IGBT selection for Tesla coils or ZCS inverters“, Kaizer Power Electronics, http://kaizerpowerelectronics.dk/tesla-coils/drsstc-design-guide/igbts/, 26.10.2020.

This external modulator sends short pulses to the gate driver, in which the coil should turn on and immediately turn off again. Such a switch-on sequence usually lasts between 30 and 300 µs. During this time, the primary resonant circuit is excited and power is transferred to the secondary resonant circuit. This results in a voltage overshoot at the toroid, which consequently leads to a discharge. The length of these signals is defined as the so-called **pulse width**. Depending on the system used, the pulse width has an influence on the size and type of the discharges. A longer pulse width and thus a longer transient phase leads to a larger power transfer and thus to stronger and longer discharges. Finally, such a pulse corresponds to a voltage discharge at the tesla transformer, which emits a characteristic and loud bang.[21]

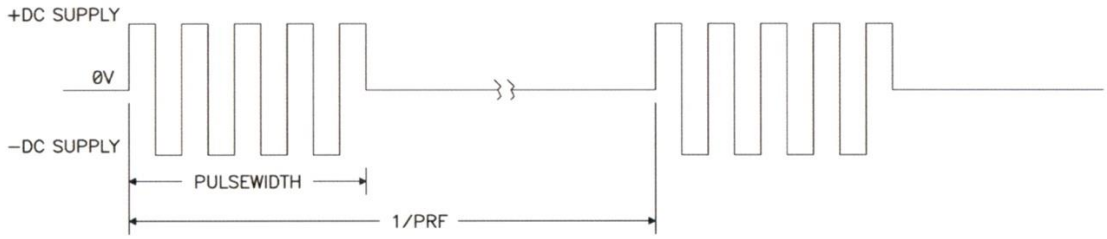

Figure 13: During the pulse width of the interrupt signal, the bus voltage is switched via the primary oscillating circuit.

Now several of these pulses can be sent to the DRSSTC in succession, which leads to regular discharges at the top load. If this happens in a periodically repeating process, we speak of a frequency. The discharges are therefore controlled at this **pulse frequency**. If this pulse frequency is between 20 Hz and 20,000 Hz, i.e. in the audible frequency range of humans, sounds can be played with the discharges. For example, if the pulse frequency is set to 440 Hz, 440 discharges per second are produced. At this frequency, the loud bangs of the individual discharges are perceived as sound. In this example, the concert pitch A (a′) will be heard.[22] [23]

The interrupter is basically an **external pulse frequency and pulse width modulator**. Figure 13 illustrates the pulse width and pulse frequency. During the duration of the pulse width, the resonant frequency of the oscillating circuit is excited. Such signals are sent by the interrupter in the form of a light pulse through a fiber optic cable to the gate driver. Without the interrupter, it would not be possible to drive

[21] „PWM - Pulsweitenmodulation“, Elektronik-Kompendium, https://www.elektronik-kompendium.de/sites/kom/0401111.htm, 16.10.2020.
[22] „Menschliches Hörvermögen im Vergleich“, Hansaton, https://www.hansaton.at/blog/hoeren-und-hoerverlust/menschliches-hoervermoegen-im-vergleich/, 14.10.2020.
[23] „PFM - Pulsfrequenzmodulation“, Elektronik-Kompendium, https://www.elektronik-kompendium.de/sites/kom/0401131.htm, 16.20.2020.

the tesla transformer. It controls the final signals for the discharges. It thus represents the last control instance by the user of the DRSSTC.[24]

Figure 14: The ready assembled interrupter in the aluminum housing.

For this work, the MIDI 2 Controller was purchased from Gao Guangyan. The MIDI 2 Controller is a simple and robust interrupter that consists of **two pre-programmed ATMEGA328P-AU microcontrollers**.[25] Because the focus of this work was not on developing an interrupter, the MIDI 2 Controller was purchased from Gao Guangyan. The finished interrupter with two outputs can be seen in Figure 14.

[24] Barnkob Mads, „Musical SSTC/DRSSTC interrupter“, Kaizer Power Electronics, http://kaizerpowerelectronics.dk/tesla-coils/musical-sstcdrsstc-interrupter/, 14.10.2020.
[25] Guangyan Gao, „Dual Channel MIDI DRSSTC Controller (MIDI2)“, Loneoceans, https://www.loneoceans.com/labs/sales/midi2/, 15.10.2020.

4 Measurement of the Secondary Voltage

To **answer the second question**, two different approaches were followed. These are methods of measuring an electrical voltage of 200,000 V, which changes sign more than 100,000 times per second.

Conventional high-voltage measuring instruments cannot be used for a Tesla transformer. In any case, an additional measuring probe on the toploaad increases the secondary capacitance and thus changes the resonant frequency of the sensitive system. Consequently, an incorrect voltage is measured which does not correspond to the fine-tuned DRSSTC. For this reason, other approaches must be taken to measure the voltage accurately and without interference. Figure 15 shows the impressive discharges whose voltage is to be measured.

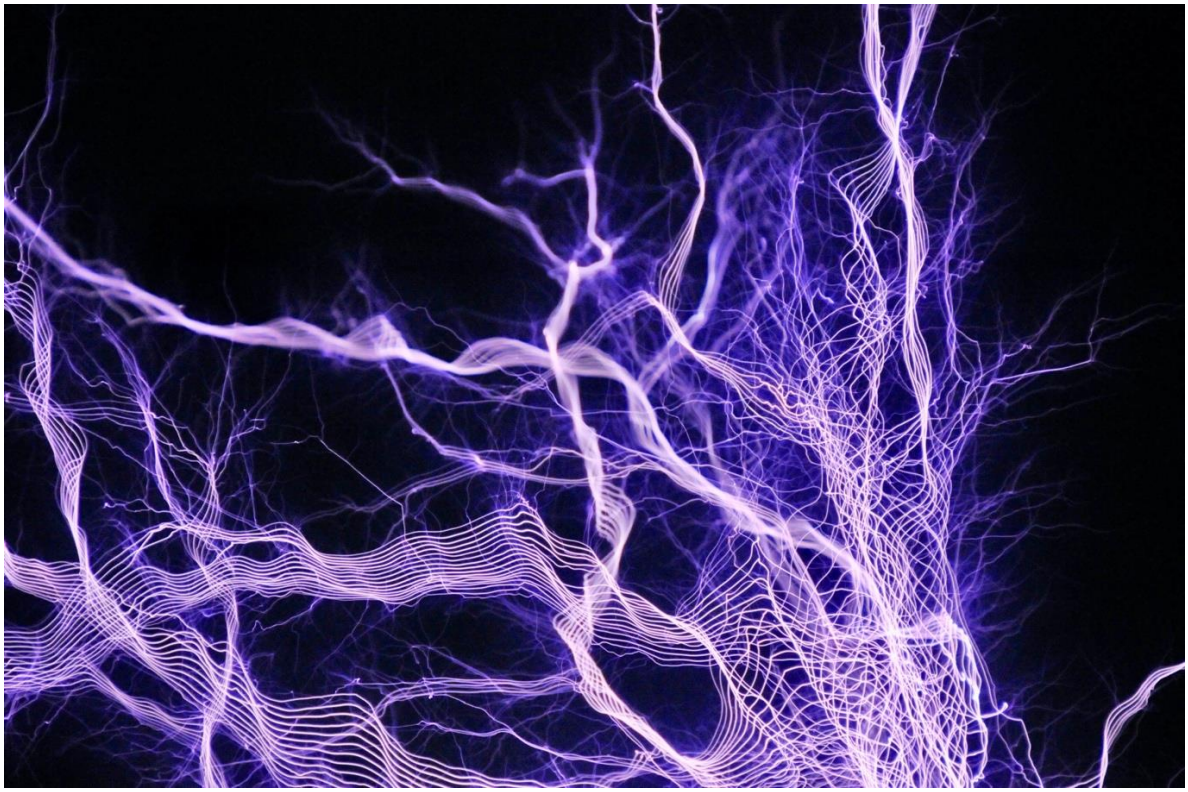

Figure 15: Close-up of the discharges to be measured.

In the following sections, two fundamentally different measurement methods for secondary voltage determination are presented. In the first approach, the secondary voltages are calculated via the measured **secondary current**. In the second experimental setup, the voltage is measured via the divider ratio using an **in-house developed measuring electrode**.

4.1 Voltage Calculation via Secondary Current Measurement

An **indirect way** to determine the voltage of a Tesla transformer is the secondary current measurement. Subsequently, the secondary voltage is calculated from the secondary currents using the following formula.[26]

$$\widehat{U}_2 = 2\pi f L_2 \hat{I}_2$$

Where L_2 is the inductance of the secondary coil in Henry, f is the resonant frequency in Herz and $\hat{I}_2$ is the amplitude current in amperes of the secondary resonant circuit.

The secondary inductance was calculated and is L_2 = 63.58 mH. To measure the **resonant frequency f and the secondary current $\hat{I}_2$**, the Wide Band Current Transformer 411 from Pearson Electronics was connected to the ground of the Tesla transformer as shown in Figure 16.

The tesla transformer was operated at a **pulse frequency of 300 Hz** and a **pulse width of approximately 60 µs**. At a pulse width of more than 60 µs, the over current detection is triggered by the gate driver. The transformer was also operated outdoors so that the environment has as little influence as possible on the secondary capacitance.

Figure 16: A current transformer was used to measure the secondary currents $\hat{I}_2$ and the resonant frequency f at ground.

[26] Färber Raphael, *Mail correspondence with author*, ETH Zürich, 27.10.2020.

The **evaluation of the measurement** results on Figure 17 show that a secondary current $\hat{I}_2$ of 3.65 A flowed through the ground with a resonant frequency f of 130.38 kHz.

The secondary voltage can now be approximately calculated:

$$\hat{U}_2 = 2\pi f L_2 \hat{I}_2 = 2\pi \cdot 130'380\ Hz \cdot 63.58 \cdot 10^{-3} H \cdot 3.65A = 190'109V$$

The amplitude voltage of the discharges is approximately **$\hat{U}_2$ = 190 kV**, which is a realistic value for a DRSSTC in this power category.[27]

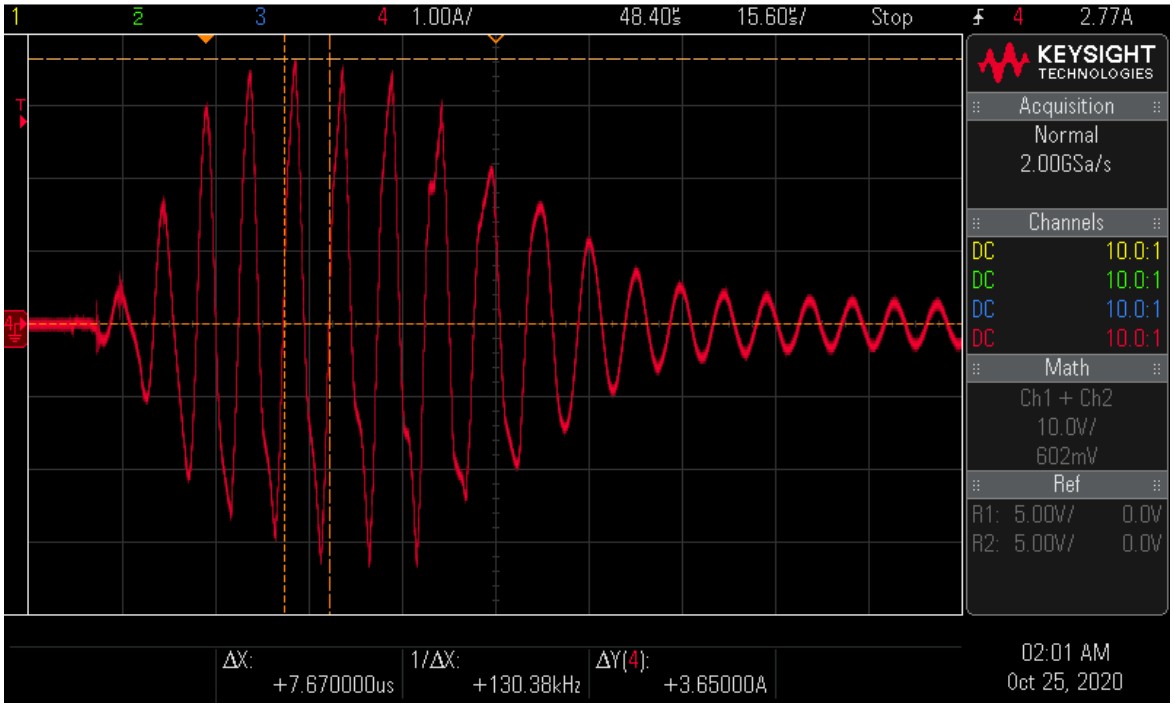

Figure 17: Measurement result of the secondary current measurement.

4.2 Voltage Measurement via Measuring Electrode

The voltage measurement via an electrode, which is placed some meters away from the Tesla transformer, shows a **fundamentally different measurement approach**. The aim is to calculate the divider ratio r between the secondary voltage U_{sec} and the measured oscilloscope voltage U_{osc}. The divider ratio r can again be multiplied by the oscilloscope voltage U_{osc} to obtain the secondary voltage U_{sec}.

This documentation is the **first known independent measurement method** to measure the secondary voltages of a Tesla transformer.

[27] Färber Raphael, *Mail correspondence with author*, ETH Zürich, 27.10.2020.

There are **three major advantages** of voltage measurement via a measuring electrode:

- There is no physical contact with the tesla transformer, which significantly interferes with its operation.
- The electrodes are cheap and easy to manufacture.
- If the values and thus the divider ratio are correct, the measuring electrode offers a very precise and reliable method of measuring secondary voltages.

Figure 18 shows a **simulation of the experimental setup** by *LTspice XVII from Analog Devices*.[28] The simulation was provided by Dr. Raphael Färber from ETH Zurich. Through it, the quantities to be measured can be estimated and the phase shift due to the coupling capacitance C_k can be investigated.

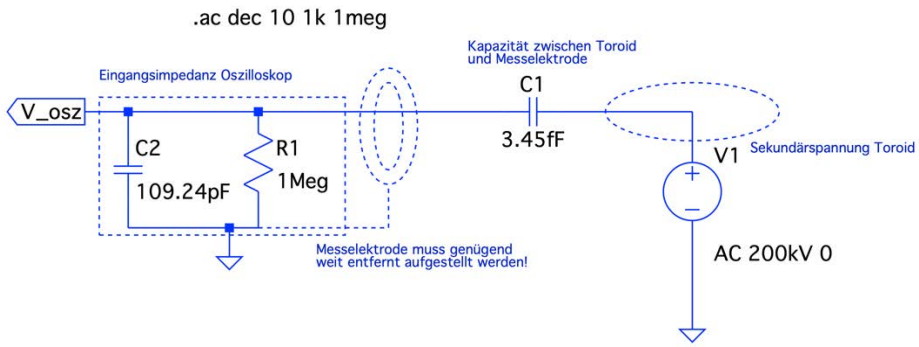

Figure 18: Simple LTspice simulation of voltage measurement via a measuring electrode.

The operation and principle of the measurement is relatively simple. The electrode is connected to the oscilloscope and consists only of a copper plate, which has a coupling capacitance C_k to the top load. The current I flowing through the impedance Z_{High} (impedance of the coupling capacitance C_k, in figure 75 C1) and input impedance Z_{Low} (R1) of the oscilloscope is constant over the whole experimental setup. The **constant current I** now allows the **divider ratio r** between the secondary voltage U_{sec} and the measured oscilloscope voltage Uosc to be calculated if the impedances Z_{Low} and Z_{High} are known.

Figure 19 shows in a frequency response plot; the simulated oscilloscope voltage U_{osc} as a solid line and the phase shift $\measuredangle r$ as a dashed line. At secondary voltages of about 200 kV, it is evident from the simulation result that the **phase shift is negligible at a resonant frequency of 130 kHz** and **voltages of about 6.6 V** can be expected.

[28] „LTspice“, Analog Devices, https://www.analog.com/en/design-center/design-tools-and-calculators/ltspice-simulator.html, 22.10.2020.

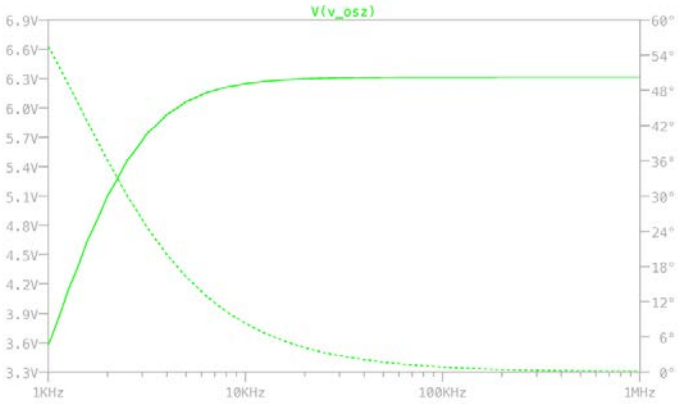

Figure 19: The simulation result of the voltage measurement via a measuring electrode.

The **experimental setup** is simple and basically consists of the measuring electrode, the connecting cable and a small gas discharge tube to protect the oscilloscope. The complete experimental setup can be seen in Figure 20. The tesla transformer can be seen in the background at a safe distance from the measuring electrode. The measuring electrode was mounted on a camera tripod and connected to the oscilloscope via a coaxial cable. In front of the oscilloscope a PCB board is connected, on which the gas discharge tube is soldered. The measured voltage is displayed on the oscilloscope. The electrode was **placed 3.5 m away** and at the **same height as the toroid**.

Figure 20: The experimental setup of the voltage measurement via a measuring electrode.

For the **measuring electrode, a PCB was developed** on which a bare and square conductor area with a side length of 15 cm is present. To protect this conductor area from leakage current or other interference signals, a grounded guard ring was placed

around the electrode. Directly behind the PCB with the measurement electrode, a second PCB was screwed on, to which the BNC connector was attached. Between the two PCBs, a small wire connects the electrode to the inner conductor of the coaxial cable, while the screws connect the guard ring to ground. The ready assembled measuring electrode can be seen on the figure 21.

Figure 21: The assembled measuring electrode on the stand from the front, back and side (fLTR).

A 91.44 cm long 50 Ω RG-174 coaxial cable from Johnson with BNC connector was used as the **connecting cable between the electrode and the oscilloscope**.[29]

To protect the oscilloscope from overvoltage, another small PCB was developed on which a **gas discharge tube** was soldered.[30] Figure 22 shows the small PCB. If the voltage on the measuring electrode is too high, it is shorted to ground, protecting the oscilloscope. There is also a slot for an optional capacitor to increase the input capacitance and thus the divider ratio. If the oscilloscope voltage is too high, it can be lowered by the additional capacitor. However, it was not needed in this experimental setup.

[29] „415-0198-036“, Mouser Electronics, https://www.mouser.ch/ProductDetail/530-415-0198-036, 14.3.2021.
[30] „B88069X2250S102“, Mouser Electronics, https://www.mouser.ch/ProductDetail/871-B88069X2250S102, 14.3.2021.

Figure 22: The small PCB is connected directly to the oscilloscope.

The **magnitude of the divider ratio |r| and the phase shift ∢r** can be derived from the coupling capacitance C_k, input capacitance C_i and input resistance R_i as follows.[31]

Here the impedance of the coupling capacitance Z_{High} is given by:

$$Z_{High} = \frac{1}{j\omega C_k}$$

The input impedance Z_{Low} of the oscilloscope is given by:

$$Z_{Low} = \left(\frac{1}{R_i} + j\omega C_i\right)^{-1} = \left(\frac{1 + j\omega R_i C_i}{R_i}\right)^{-1} = \frac{R_i}{1 + j\omega R_i C_i}$$

The current sought flows through both impedances, so they are added like two resistors in a series circuit:

$$Z_{total} = Z_{High} + Z_{Low} = \frac{1}{j\omega C_k} + \frac{R_i}{1 + j\omega R_i C_i}$$

Consequently, the flowing current I is given by:

$$I = \frac{U_{sek}}{Z_{total}} \Rightarrow U_{sek} = Z_{total} I$$

The measured voltage at the oscilloscope U_{osc} is against by the current I:

$$U_{osc} = Z_{Low} I = Z_{Low} \frac{U_{sek}}{Z_{total}}$$

[31] Färber Raphael, *Mail correspondence with author*, ETH Zürich, 3.3.2021.

As a result, the divider ratio is given by:

$$r = \frac{U_{sec}}{U_{osc}} = \frac{Z_{total}}{Z_{Low}} = \frac{1 + j\omega R_i C_i}{j\omega R_i C_k} + 1 = 1 + \frac{C_i}{C_k} + \frac{1}{j\omega R_i C_k}$$

The magnitude |r| and the phase shift ∢r is thereby:

$$|r| = \sqrt{\left(1 + \frac{C_i}{C_k}\right)^2 + \left(\frac{1}{\omega R_i C_k}\right)^2} \approx 1 + \frac{C_i}{C_k}, falls\ \omega R_i C_k \gg 1$$

$$\measuredangle r = -arctan\left[\frac{\frac{1}{\omega R_i C_k}}{1 + \frac{C_i}{C_k}}\right] \approx 0, falls\ \omega R_i C_k \gg 1$$

Compared with the simulation from figure 18 and 19, the result agrees with the derivation of the divider ratio and the phase shift.

From the technical specifications, the **input resistance R_i** of the oscilloscope can be taken. This is 1 MΩ.

To determine the **input capacitance C_i**, the individual capacitances of the experimental setup must be added together. The individual capacitances are arranged in parallel from the measuring electrode to ground and can thus be added together to obtain the total input capacitance C_i. The oscilloscope has an input capacitance of 16 pF. The RG-174 coaxial cable has an inherent capacitance of about 101.97 pF per meter. Thus, the 91.44 cm long coaxial cable with BNC connector has a capacitance of 93.24 pF. Consequently, the input capacitance is C_i:[32]

$$C_i = C_{Kabel} + C_{Osci} = 93.24\ \text{pF} + 16\ \text{pF} = 109.24\ \text{pF} = 1.0924 \cdot 10^{-10}\ F$$

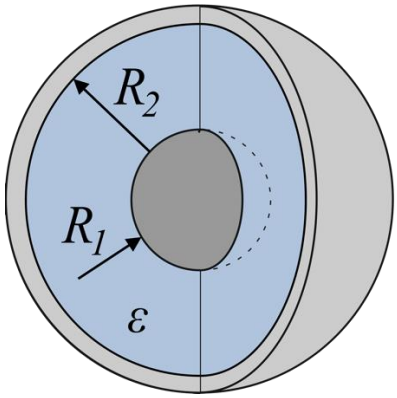

Figure 23: Spherical capacitor with radii R_1 and R_2.

[32] „Parallelschaltung von Kondensatoren“, Elektronik-Kompendium, https://www.elektronik-kompendium.de/sites/slt/1006091.htm, 17.3.2021.

The **coupling capacitance C_k** can be estimated mathematically by an approximation of a spherical capacitor. Here, in Figure 23, the radius R_1 is the radius of the toroid R_T and the radius R_2 is the distance from the center of the toroid to the measuring electrode R_M. The electric field constant ε_0 is 8.854 · 10-12 As/Vm. The capacitance of a spherical capacitor C is given by:[33]

$$C = \frac{4\pi\varepsilon_0}{\frac{1}{R_T} - \frac{1}{R_M}}$$

The surface of the sphere is given by:

$$A = 4\pi {R_M}^2$$

The measuring electrode area A_M is a fraction of the large sphere area:

$$C_k = \frac{A_M}{4\pi {R_M}^2} \cdot \frac{4\pi\varepsilon_0}{\frac{1}{R_T} - \frac{1}{R_M}}$$

The measuring electrode has a square size of 15 cm side length. The measuring electrode area AM is therefore 0.0225 m^2. As already mentioned in the experimental setup, the distance between the center of the toroid and the measuring electrode was 3.5 m. The toroid has a diameter of 40 cm. Because the secondary capacitance is basically slightly increased by the discharges, this approximation assumes that the toroid is a sphere with a radius of 0.2 m. This means that the toroid is a sphere with a radius of 0.2 m. This is a sphere with a radius of 0.2 m. Consequently, this corresponds to a coupling capacitance C_k of:

$$C_k = \frac{0.0225\ m^2}{4\pi(3.5\ m)^2} \cdot \frac{4\pi\varepsilon_0}{\frac{1}{0.2\ m} - \frac{1}{3.5\ m}} \approx 3.450 \cdot 10^{-15}\ F = 3.450\ fF$$

[33] Färber Raphael, *Mail correspondence with author*, ETH Zürich, 3.3.2021.

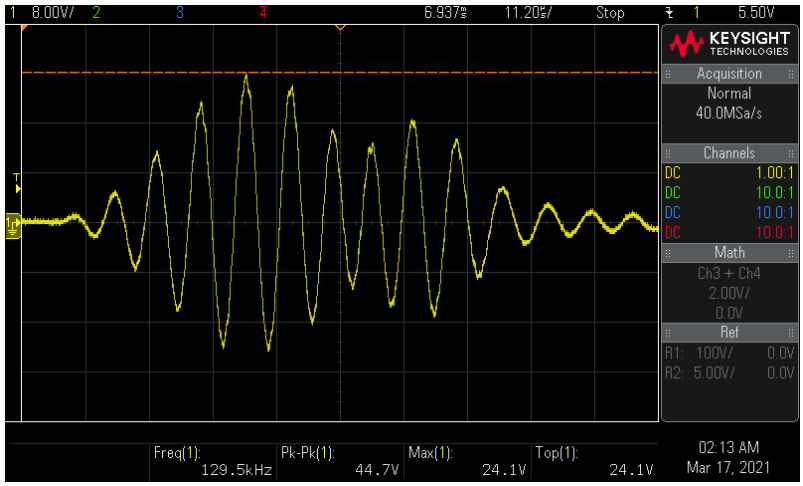

Figure 24: The voltage measurement at the measuring electrode.

The tesla transformer was operated with a **pulse frequency of 300 Hz** and a **pulse width of about 60 µs** during the measurement. The same pulse width and frequency were also used for measuring the voltage via the secondary current measurement. The transformer was also operated outdoors so that the environment had as little influence as possible on the secondary capacitance.

The **evaluation of the measurement result** on figure 24 shows that the resonant frequency f is about 130 kHz and the measured voltage peaks of U_{osc} are about 24 V.

The divider ratio |r| can now be calculated from the calculated capacitances, the measured resonant frequency of 130 kHz and the input resistance R_i of 1 MΩ:

$$|r| = \sqrt{\left(1 + \frac{C_i}{C_k}\right)^2 + \left(\frac{1}{\omega R_i C_k}\right)^2}$$

$$= \sqrt{\left(1 + \frac{1.0924 \cdot 10^{-10}\,F}{3.450 \cdot 10^{-15}\,F}\right)^2 + \left(\frac{1}{2\pi \cdot 1.3 \cdot 10^5\,Hz \cdot 10^6\,Ohm \cdot 3.450 \cdot 10^{-15}\,F}\right)^2}$$

$$\approx 31'666.76$$

The secondary voltage U_{sek} is now given by multiplying the divider ratio |r| by the oscilloscope voltage U_{osc}:

$$U_{sek} = |r| \cdot U_{osc} = 31'666.76 \cdot 24\,V \approx 760'000\,V$$

With this measurement method, the calculated secondary voltage across the divider ratio is **U_{sek} = 760,000 V**, which is a very high and rather unrealistic value for a DRSSTC of this size.

5 Discussion

The voltage calculation via the secondary current resulted in a secondary voltage of about **200 kV**, while the new method of voltage measurement yielded a value of about **750 kV**.

It is noticeable that the results differ greatly from each other. After consultation with Dr. Raphael Färber of ETH Zurich, the secondary voltage of about **200 kV is much more realistic**.

Since the 750 kV is far above a realistic voltage value, **consequently the divider ratio |r| must be too high**. Accordingly, either the input capacitance C_i is too large or the coupling capacitance C_k is too small. The **source of error** probably lies in the coupling capacitance C_k being too small and not in the input capacitance Ci being composed of known values. There are two main reasons why **approximating the coupling capacitance C_k across a spherical capacitor is not very accurate**:

- The approximately 1 m long **discharges** exiting the toroid increase the surface area of the topload due to their strong branching and consequently increase the coupling capacitance C_k.
- The **coil former itself** also contributes to the coupling capacitance C_k.

Thus, **voltage measurement via the electrode** proves to be much **less reliable** compared to voltage calculation via the secondary current. The reason lies in the quantities to be estimated, which can strongly falsify the result. However, if the capacitances are known, voltage measurement via the electrode offers a reliable alternative, which is additionally safer than secondary current measurement.

However, the measuring electrode can be used not only for secondary voltage measurement, but also to further **investigate the voltage curve of the discharges**. For many investigations the absolute value of the voltage is not relevant. The voltage curve can be used, for example, to investigate the influence of the discharge direction or the branching of the primary coil.

Finally, **both questions were answered comprehensively**. At the same time, the documentation on voltage measurement with the measuring electrode is a completely new approach to analyzing secondary voltages from a Tesla transformer. There are many more phenomena that could be studied in more detail using this high voltage generator.

6 References

6.1 Literature Sources

McCauley Daniel, *DRSSTC Building the Modern Day Tesla Coil* (United States of America: Lulu Press, 2006).

Albach Manfred, *Elektrotechnik* (München: Pearson Deutschland GmbH, 2020).

6.2 People

Färber Raphael, Mail correspondence with author, ETH Zürich.

6.3 Scientific Papers

Gadola Robin, Stamm Jonas, Uschatz Cédric, *Entwicklung der Gate-Treiber Stufe für eine Audiomodulierte Teslaspule*, Gruppenarbeit Herbstsemester 16/17, ETH Zürich.

6.4 Internet Sources

„415-0198-036“, Mouser Electronics, https://www.mouser.ch/ProductDetail/530-415-0198-036, 14.3.2021.

„B88069X2250S102“, Mouser Electronics, https://www.mouser.ch/ProductDetail/871-B88069X2250S102, 14.3.2021.

„CM300DY-24H“, Digi-Key Electronics, https://www.digikey.com/en/products/detail/powerex-inc/CM300DY-24H/1996275, 26.10.2020.

„LTspice“, Analog Devices, https://www.analog.com/en/design-center/design-tools-and-calculators/ltspice-simulator.html, 22.10.2020.

„Menschliches Hörvermögen im Vergleich“, Hansaton, https://www.hansaton.at/blog/hoeren-und-hoerverlust/menschliches-hoervermoegen-im-vergleich/, 14.10.2020.

„Nikola Tesla“, Who’s who, https://whoswho.de/bio/nikola-tesla.html, 22.11.2021.

„Parallelschaltung von Kondensatoren“, Elektronik-Kompendium, https://www.elektronik-kompendium.de/sites/slt/1006091.htm, 17.3.2021.

„PFM - Pulsfrequenzmodulation“, Elektronik-Kompendium, https://www.elektronik-kompendium.de/sites/kom/0401131.htm, 16.20.2020.

„Tesla's Tower at Wardenclyffe“, Tesla Science Center, https://teslasciencecenter.org/history/tower/, 22.11.2021.

„Teslaspule: Geschichte, Funktionsprinzip, Anwendung“, hilfreich.de, http://www.hilfreich.de/teslaspule-geschichte-funktionsprinzip-anwendung_7868, 22.11.2021.

Barnkob Mads, „IGBT selection for Tesla coils or ZCS inverters“, Kaizer Power Electronics, http://kaizerpowerelectronics.dk/tesla-coils/drsstc-design-guide/igbts/, 26.10.2020.

Barnkob Mads, „Musical SSTC/DRSSTC interrupter“, Kaizer Power Electronics, http://kaizerpowerelectronics.dk/tesla-coils/musical-sstcdrsstc-interrupter/, 14.10.2020.

Bell Steve, „Secondary Coil“, DeepFriedNeon, http://deepfriedneon.com/tesla_secondary.html, 3.10.2020.

Gadola Robin, Stamm Jonas, Uschatz Cédric, Entwicklung der Gate-Treiber Stufe für eine Audiomodulierte Teslaspule, Gruppenarbeit Herbstsemester 16/17, ETH Zürich.

Guangyan Gao, „Dual Channel MIDI DRSSTC Controller (MIDI2)“, Loneoceans, https://www.loneoceans.com/labs/sales/midi2/, 15.10.2020.

Guangyan Gao, „UD 2.7“, Loneoceans, https://www.loneoceans.com/labs/ud27/, 12.10.2020.

Tesla Nikola, „System Of Electric LIghting“, Google Patents, https://patents.google.com/patent/US454622, 12.10.2020.

Ward Steve, „New DRSSTC Driver (2008 and now 2009)“, SteveHV, https://www.stevehv.4hv.org/new_driver.html, 13.10.2020.

6.5 Illustration Sources

Figure 25: Magnetically coupled primary and secondary resonant circuit via inductances L_{pri} and L_{sec}: Wackernagel Daniel, Assembly and Testing of an Audio-Modulated Solid-State Tesla Coil, Semester Thesis, ETH Zürich, S. 1.

Figure 26: Primary and secondary voltage: „HOW A TESLA COIL WORKS“, oneTesla, http://onetesla.com/tutorials/how-a-tesla-coil-works, 28.10.2020.

Figure 27: Primary oscillating circuit with C_{bus} as DC voltage source and the switches S1 and S2, which switch it via the oscillating circuit: Wackernagel Daniel, Assembly and Testing of an Audio-Modulated Solid-State Tesla Coil, Semester Thesis, ETH Zürich, S. 2.

Figure 28: Schematic representation of a DRSSTC: McCauley Daniel, DRSSTC Building the Modern Day Tesla coil (United States of America: Lulu Press, 2006), S. 195.

Figure 29: An audio modulated DRSSTC with medium power output: Illustration by author.

Figure 30: Simple LTspice simulation of a DRSSTC with half-bridge circuit: Illustration by author.

Figure 31: The DC voltage in blue keeps on swaying the sinusoidal current through the primary coil in green: Illustration by author.

Figure 32: The DRSSTC with the eye-catching and characteristic secondary coil: Illustration by author.

Figure 33: Basic operation of the gate driver in schematic representation: McCauley Daniel, DRSSTC Building the Modern Day Tesla coil (United States of America: Lulu Press, 2006), S. 196.

Figure 34: The completely assembled UD 2.8 on the self-designed circuit board: Illustration by author.

Figure 35: A CM300DY-24H IGBT half bridge module from Powerex: Illustration by author.

Figure 36: The CM300DY-24H IGBT module mounted on the grounded heat sink: Illustration by author.

Figure 37: During the pulse width of the interrupt signal, the bus voltage is switched via the primary oscillating circuit: McCauley Daniel, DRSSTC Building the Modern Day Tesla coil (United States of America: Lulu Press, 2006), S. 104.

Figure 38: The ready assembled interrupter in the aluminum housing: Illustration by author.

7 Appendix

The appendix can be accessed digitally on the Internet via the following URL:

https://drive.google.com/drive/folders/1Ie4WvCgWcIhyMEIzKRgoVSQzY8EVamUY?usp=sharing.

There are more pictures, videos, measurements and the CAD drawings of the plexiglass parts stored on the Google Drive folder.

【評語】100040

The work in realizing an audio modulated Tesla coil is well conducted. The author has put a lot of thought in designing and testing the high frequency circuits. For characterization, the author may consider using electro-optical effect to measure the high voltage at high frequency.

In the current report, only one figure (Figure 24) shows the experimental results. More experimental validation is suggested.

Note that there are similar works using Tesla coil with audio modulation, such as https：//youtu.be/C8wpX4QvtNc. The author may want to distinguish his uniqueness with a comparison to other similar works.